Journal of the European Ceramic Society 23 (2003) 791–799

www.elsevier.com/locate/jeurceramsoc

Microwave reaction bonding of silicon nitride using an inverse temperature gradient and ZrO_2 and Al_2O_3 sintering additives

J.G. Fisher*, S.K. Woo, K. Bai, I.S. Han, K.S. Lee, K.S. Hong, D.W. Seo

Energy Materials Research Team, Korea Institute of Energy Research, 71-2 Jang-dong, Yusong-ku, Taejon 305-343, Republic of Korea

Received 29 August 2001; received in revised form 27 May 2002; accepted 16 June 2002

Abstract

Si preforms containing Si_3N_4, Al_2O_3 and ZrO_2 sintering additives were produced via an aqueous gelcasting route with 45 vol.% dry matter solids loading. Samples up to 10 mm thick could be produced without cracking. Microwave nitridation of the preforms was carried out using a fiberboard insulation box without packing powders in order to effect an inverse temperature gradient. Nitridation began at ~800 °C and up to 40% nitridation was achieved by nitriding at 930–950 °C. Nitriding at higher temperatures caused a decrease in the amount of nitridation. All the samples displayed an inverse temperature gradient. In the centre of the samples, overheating occurred, which led to sintering and melting. Sample melting could be reduced by reducing the nitridation gas pressure from 0.2 to 0.1 MPa.

Keywords: Defects; Microwave processing; Optical microscopy; Si_3N_4

1. Introduction

Si_3N_4 ceramics have potential for high-temperature structural applications such as turbine rotors and shrouds[1] but the high cost of conventionally sintered Si_3N_4 ceramics has limited their use. As a consequence, much research has been devoted to reaction bonding, a way of producing Si_3N_4 ceramics using relatively cheap Si powder and N_2 gas instead of expensive α-Si_3N_4 powder.

Reaction bonding of Si is usually carried out in conventional furnaces. However, microwave reaction bonding offers several potential advantages. In conventional reaction bonding, the pores in the exterior of the preform close up before complete nitridation has taken place in the interior.[2] This prevents the diffusion of N_2 into the preform, and limits the green density and size of the Si preform than can be nitrided. Microwave processing has the advantage of heating the sample volumetrically, so that it is always hotter in the center than at the edges. This can allow nitridation to take place in the center of the preform first. Research has also shown that nitridation using microwave heating takes place at slightly lower temperatures (~50 °C) and at faster rates than with conventional heating.[3,4]

Usually, Si samples are packed in Si_3N_4 packing powder during microwave nitridation if a follow up sintering step is to be carried out.[5,6] This is done in order to minimize decomposition of Si_3N_4 during sintering. However, this will reduce the inverse temperature gradient across the samples. In the present study a minimum of insulation was used in order to observe the effect of a large inverse temperature gradient upon the nitridation behavior of Si samples.

If the reaction bonded Si_3N_4 is to be subsequently sintered, then sintering additives have to be included. Because of the covalent nature of the Si–N bond, Si_3N_4 cannot be sintered by solid-state diffusion, and so must use liquid phase sintering.[7] Densification takes place via a solution-reprecipitation process. The additives react with the SiO_2 coating on the α-Si_3N_4 powder to form a liquid phase, which then reacts with the α-Si_3N_4. β-Si_3N_4 precipitates from the liquid. The final microstructure of the ceramic consists of acicular or elongated

---

* Corresponding author at current address: Department of Materials Science and Engineering, Korea Advanced Institute of Science and Technology, 373-1 Kusong-dong, Yusong-Ku, Taejon 305-701, Republic of Korea.

E-mail address: johnfisher@kaist.ac.kr (J.G. Fisher).

0955-2219/02/$ - see front matter © 2002 Elsevier Science Ltd. All rights reserved.
PII: S0955-2219(02)00196-6

β-Si_3N_4 grains surrounded by a grain boundary phase whose composition depends on the sintering additives used.

The most common sintering additives used are Al_2O_3 and Y_2O_3. However, Y_2O_3 is expensive. Finding a cheaper sintering additive would help to reduce the cost of producing Si_3N_4 ceramics so in this study an alternative to Y_2O_3 was chosen. To be effective, the additive should both promote densification of the ceramic and produce a refractory grain boundary phase.[8] The additives should also not cause Si_3N_4 decomposition to occur by reaction of the additive with Si_3N_4.[9]

A possible replacement for Y_2O_3 is ZrO_2. Addition of ZrO_2 is known to increase the melting temperature and corrosion resistance of glasses. The eutectic point of the Al_2O_3–ZrO_2 system is 1710 ± 10 °C at 42.6 wt.% ZrO_2.[10] ZrO_2 efficiently absorbs microwaves at temperatures above 800 °C,[11] which would be beneficial to sintering. In addition, relatively little work has been carried out using ZrO_2 as a sintering additive. Therefore, in this paper the effectiveness of ZrO_2 as a sintering aid for sintered reaction bonded Si_3N_4 will be discussed.

Negita,[9] in a comparison of the standard free energies for oxidation reactions of Si_3N_4 at 2000 K with those of metals and metal nitrides, found that both Al_2O_3 and ZrO_2 should be effective sintering aids. Al_2O_3 is commonly used as a sintering aid in combination with oxides such as Y_2O_3 and MgO. Rice and McDonough[12] successfully used ZrO_2 and $ZrSiO_4$ as sintering aids for hot-pressed Si_3N_4. However, the formation of AlN and ZrN during sintering has been reported,[13,14] indicating that decomposition of Si_3N_4 occurred. Inomata et al.[15] observed effective densification of a Si_3N_4 powder containing 2–5 wt.% Al_2O_3 plus 3–5 wt.% ZrO_2.

2. Experimental

2.1. Sample preparation

Samples of composition Si–10 wt.% Si_3N_4–6.9 wt.% Al_2O_3–5.1 wt.%ZrO_2 were produced. Al_2O_3 (Sumitomo Chemical Co., Japan) and ZrO_2 (Tosoh Corp., Japan) sintering additives were added in the same ratio as that of the eutectic composition in the Al_2O_3–ZrO_2 binary system. The Si powder used was Sicomil 2F (Permascand, Sweden). Details of this powder are given in Table 1. α-Si_3N_4 (Sumitomo Chemical Co., Japan) was added to promote growth of α-Si_3N_4 during reaction bonding. Batches were ball milled for 24 h in acetone using ZrO_2 milling media and polypropylene jars. After milling, batches were dried in an oven.

Table 1
Composition and size distribution of Si powder

% Fe	% Al	% Ca	% C	d_{10} (μm)	d_{50} (μm)	d_{90} (μm)
0.47	0.16	0.06	0.05	0.7	3.2	6.8

Samples were produced via the gelcasting route. For the gel-casting solution, a composition developed by Janney et al.[16] was used. 12.9 wt.% methacrylamide was used as the monomer. 2.1 wt.% *N*,*N*′-methylene bisacrylamide was used as the cross-linking agent. 1 wt.% Darvan C (R. T. Vanderbilt Co., USA) was used as dispersant. Distilled water was used as the solvent. 250 μl of 10 wt.% ammonium persulfate soln. per 100 ml of premix solution was used as initiator, with 25 μl of *N*,*N*,*N*′ ,*N*′-tetramethylethylenediamine as catalyst.

The premix solution containing the solvent, monomer, cross-linking agent and dispersant was premixed for 1 h. The batch was then added to the solution and stirred in an open vacuum flask for 24 h using a mechanical stirrer. A solids loading of 45 vol.% dry matter was used. The slurry was then vacuum de-aired, initiator and catalyst were added and the slurry cast into plastic moulds. The dimensions of the moulds were 31 mm×31 mm×29 mm. Oleic acid was used as the mould release agent. Gelation was performed at 60 °C. Gelation took between 15 and 30 min. The samples were left in the moulds under ambient conditions for 1–2 days before removal. After removal, samples were left to dry for 2–3 days under ambient conditions.

After the samples had dried, the binder was burnt out by heating the samples to 650 °C at a heating rate of 1 $^\circ C\ min^{-1}$ holding the samples at 650 °C for 1 h and then cooling the samples to room temperature at a rate of 2.5 $^\circ C\ min^{-1}$.

The finished samples were 31 mm in length and 31 mm in width. Sample thickness varied between 10 and 12 mm. Sample weight varied between 10 and 12 g, depending on the thickness of the sample.

2.2. Nitridation studies

Samples were nitrided in a multimode furnace consisting of a steel cylindrical cavity 60 cm in length and 45.5 cm in diameter. Microwave energy is supplied by a 6 kW 2.45 GHz microwave generator (Cober, USA) and enters the furnace through a port in one end of the cavity. A mode stirrer is positioned at this port. Samples are placed on a table in the center of the cavity.

Samples were insulated using boxes made from Al_2O_3 fiberboard insulation. Sample temperature was measured by an infrared pyrometer through a hole drilled through one of the walls of the fiberboard box. A PID controller linked to the pyrometer controlled the temperature. The top face of the box was level with the bottom edge of the microwave port.

A box made from 25 mm-thick 1200 °C fiberboard was used as insulation. The dimensions of the internal cavity of this box were 150 mm×150 mm× 100 mm. A

115 mm×115 mm×8 mm Al_2O_3 tray was placed on the fiberboard base to protect it. Samples were then stacked vertically on top of a 40×40 mm×6 mm BN setter plate. Seven samples were used in each run. The top and bottom samples were discarded after each run. The pyrometer was focused on the third and fourth samples in the stack. The samples were placed in the centre of the fiberboard box, at the focal point of the pyrometer. Samples were not packed in insulating powder. Sample layout is shown in Fig. 1.

2.3. Nitridation conditions

$Si–Si_3N_4–ZrO_2–Al_2O_3$ samples were heated at a rate of 5 °C min^{-1} to the nitridation temperature, held at that temperature for 1 h, and then cooled at a rate of 5 °C min^{-1} to room temperature. Nitridation temperatures of 800, 840, 850, 860, 870, 880, 900, 910, 925 and 940 °C were used. A pressure of 0.2 MPa was used for these runs. Samples were also nitrided at 840 and 850 °C for 1 h under 0.1 MPa pressure. Some batches were also nitrided for 2 and 5 h at 850 °C under 0.1 MPa pressure. One batch was also nitrided at 925 °C for 1 h under 0.5 MPa pressure. In all runs, N_2–10% H_2 was used as the nitriding gas.

Multi-stage nitridation treatments were also carried out. Samples were nitrided under 0.1 MPa pressure. Samples were initially heated at 5 °C/min to 850 °C and nitrided at 850 °C for 1 h. The temperature was then increased by 50 °C intervals at a rate of 0.5 °C/min until the maximum nitridation temperature was reached. After each 50 °C interval, the samples were held at constant temperature for 1 h. So, for example, a batch whose maximum nitridation temperature was 950 °C would have been held at 850, 900 and finally 950 °C, each for 1 h. Samples were cooled at a rate of 5 °C/min.

2.4. Sample characterization

Samples were weighted before and after nitridation. A sample whose weight has increased by 66.5% is considered to be fully nitrided.[17] Sections of the samples were prepared for optical microscopy. Scanning electron microscopy (SEM) was also carried out on some samples. X-ray powder diffraction (XRD) was carried out on samples to determine the phases.

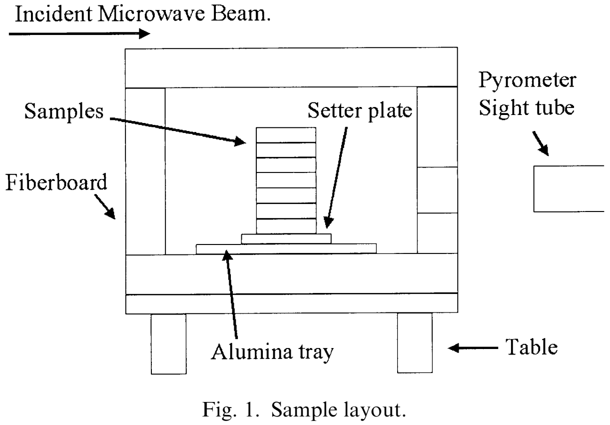

Fig. 1. Sample layout.

3. Results and discussion

3.1. Gelcasting

Crack-free samples up to 1-cm thick could be obtained. Occasionally, samples contained cracks. Both internal cracks and cracks running from the surface of the samples were present. The density of the $Si–Si_3N_4–Al_2O_3–ZrO_2$ samples was 1.31 ± 0.01 g cm^{-3}, 48% of the theoretical density. The density of the gelcast samples (as a percentage of the theoretical density) was lower than those of other workers. Maria et al.[18] record a green density of 56.3% TD for their gelcast samples, although they did not state the solids loading (dry matter content) of their slurry.

Samples often contained bubbles. Si powder particles are usually coated with a thin film of oxide.[19] Ball milling of the Si powder will have produced fresh surfaces, which could then react with the aqueous premix solution to form hydrogen gas and a film of SiO_2 on the Si powder particles.[20] These bubbles were only partially removed during de-airing. This could be seen by comparing normal $Si–Si_3N_4–ZrO_2–Al_2O_3$ samples with samples in which the vacuum de-airer had not functioned correctly. The samples that had not been de-aired contained large air bubbles several mm in diameter. The samples that had been de-aired contained smaller bubbles $\leqslant 1$ mm in diameter.

3.2. Microwave nitridation—general appearance of samples

Nitrided samples appeared grey on their side faces. The top and bottom faces of the samples were generally grey-white, often with light and dark rings. The edges of these faces were grey. Sometimes swelling and melting could be seen on the top faces of the samples.

When the samples were sectioned, the centre of the samples was often grey-white in colour. Sometimes this grey-white region extended from the center of the sample. Sometimes, it formed an arc spreading down from the top face of the sample. The remaining part of the sample was dark grey in colour, with 2–3 mm thick light grey bands at the edges of the sample.

Samples at the top of the stack show less pronounced discoloration. Often the white regions visible in samples from the bottom of the stack are absent in samples from the top of the stack. Melting is also generally less severe in samples from the top of the stack.

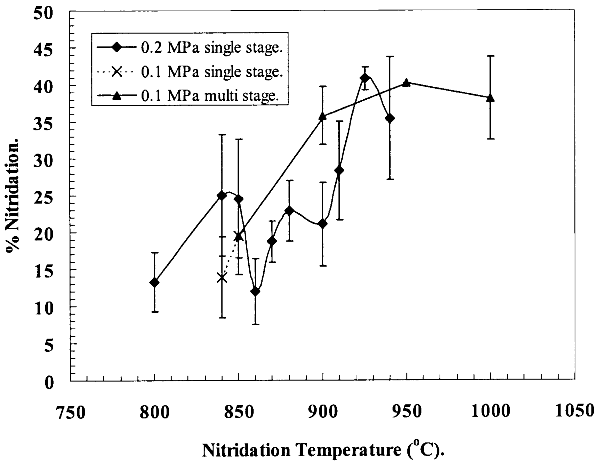

Fig. 2. Variation of the percentage of nitridation of Si–Si_3N_4–ZrO_2–Al_2O_3 samples as a function of the sintering temperature.

3.3. Single stage nitridation runs

The nitridation behavior of the single stage samples is shown in Fig. 2. For samples nitrided under 0.2 MPa, the amount of nitridation increased with temperature between 800 and 850 °C. At 860 °C, the amount of nitridation dropped and then increased with nitridation temperature until 925 °C, although the increase was not smooth. Above 925 °C, the amount of nitridation began to drop.

A nitridation temperature of 940 °C was initially chosen as it was thought that nitridation at this temperature would be slow enough to avoid sample overheating and melting. However, nitridation at this temperature was rapid enough to cause melting so the nitridation temperature was progressively lowered in order to find a nitridation temperature at which no melting took place. Unfortunately, melting took place even at temperatures as low as 800 °C.

There was a variation in the amount of nitridation between samples in the same batch. In some cases, especially at low and high temperatures, the variation in nitridation between samples in the same batch can be upto 7%. Generally, the third and fourth samples in the stack showed less nitridation than the other samples. This was because they were level with the hole in the insulation that the pyrometer sighted through, and so would loose more heat than the other samples.

All the samples nitrided under 0.2 MPa pressure displayed Si melting. Melting appears either as blobs of Si or in cracks in the sample. Other cracks in the sample are white in colour but show no melting. The second and third samples in the stack suffered the severest melting. However when samples were nitrided at 800 °C only the bottom two samples showed any melting.

Reducing the furnace gas pressure from 0.2 to 0.1 MPa caused a reduction in the nitridation rate. Samples nitrided under 0.1 MPa pressure also suffered less melting. In these samples, blobs of melted Si sometimes appeared in cracks in the sample, usually near the top face of the sample. Some samples suffered no melting. However, the second and third samples in the stack usually showed some melting.

The samples nitrided under 0.5 MPa at 925 °C suffered severe melting in all of the samples except the top one. These samples showed 34±15% nitridation.

Samples were nitrided at 850 °C under 0.1 MPa pressure for different times. The results are shown in Fig. 3. The amount of nitridation did not increase significantly with time.

3.4. Multi-stage nitridation runs

The results of the multi-stage nitridation treatments under 0.1 MPa pressure are shown in Fig. 2. Up to 40% nitridation could be achieved by nitriding samples upto a maximum temperature of 950 °C. After this the amount of nitridation began to fall off. The batch nitrided at a maximum temperature of 950 °C also showed less variation between samples in the amount of nitridation (a standard deviation of 0.9%, whereas the batches nitrided at other temperatures showed standard

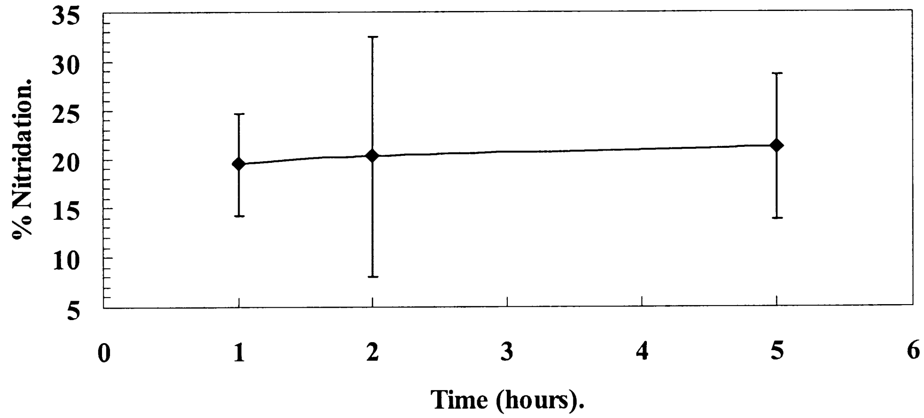

Fig. 3. Nitridation behavior of Si–Si_3N_4–ZrO_2–Al_2O_3 samples nitrided at 850 °C under 0.1 MPa pressure.

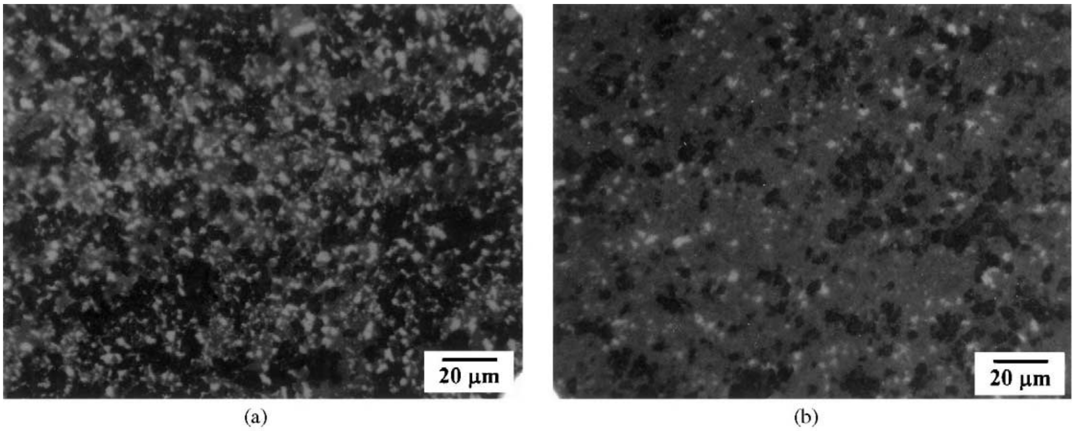

(a) (b)

Fig. 4. (a) Edge of sample nitrided at 925 °C for 1 h under 0.2 MPa pressure (single stage run). (b) Centre of sample nitrided at 925 °C for 1 h under 0.2 MPa pressure (single stage run).

deviations of 3.9–5.6%). These samples suffered less melting than samples nitrided under 0.2 MPa. In these runs, the second and third samples in the stack always showed melting. The other samples sometimes showed small amounts of melting in cracks in the samples.

At temperatures of 850 °C or below, samples nitrided under 0.1 MPa pressure showed less nitridation than samples nitrided at 0.2 MPa. This agrees with Heinrich,[21] who found that decreasing nitrogen partial pressure reduced the reaction rate. Between 850 and 900 °C, samples nitrided under 0.1 MPa pressure show more nitridation than the samples nitrided under 0.2 MPa. This is due to the lack of a reaction inhibiting oxynitride phase in the samples nitrided under 0.1 MPa, as shown in the XRD results. The samples nitrided under 0.1 MPa also suffer less weight loss when nitrided at high temperatures. In both cases, whether under 0.1 or 0.2 MPa, nitridation began to drop off after 40% nitridation occurred. This could be due to vaporization of Si at the higher nitridation temperatures.[23] The addition of ZrO_2 and Al_2O_3 as sintering additives appears to have had a detrimental effect on the maximum amount of nitridation.

The samples nitrided under 0.5 MPa pressure suffered worse melting than samples nitrided under 0.2 or 0.1 MPa pressure. This is due to the increase in nitridation rate caused by the increase in gas pressure. The $Si \rightarrow Si_3N_4$ reaction is exothermic and if the reaction proceeds too quickly then melting will occur. This problem is further compounded by the use of microwaves as the power source. Hot areas of the sample preferentially absorb microwaves over cooler areas, which can lead to thermal runaway.

3.5. Optical and scanning electron microscopy

Optical micrographs of a sample nitrided at 925 °C for 1 h under 0.2 MPa pressure are shown in Fig. 4(a) and (b). The outside edge of the sample, Fig. 4(a), consists of white un-nitrided Si particles, gray Si_3N_4 and black porosity. As in samples nitrided at lower temperatures, large amounts of unreacted Si are present. In the bulk of the sample, Fig. 4(b), more nitridation has taken place. This sample was taken from the top of the stack. Samples lower in the stack showed even more nitridation.

Micrographs of samples nitrided in a two-stage treatment (1 h at 850 °C, followed by 1 h at 900 °C) are shown in Fig. 5(a) and (b). Fig. 5(a) is taken from the bulk of a sample at the base of the stack. Very little residual Si is visible. In the very centre of this sample, Fig. 5(b), the microstructure is coarser and more residual Si is visible. Sintering between Si particles has also taken place.

A scanning electron micrograph of the fracture surface of an un-nitrided $Si–Si_3N_4–ZrO_2–Al_2O_3$ preform sample is shown in Fig. 6. The microstructure consists of angular Si particles. Porosity and pore channels can be seen between the Si particles. The Si particles are between 2 and 4 μm in diameter. Smaller sub-micron particles are clinging to the larger particles.

Scanning electron micrographs of the fracture surface of a $Si–Si_3N_4–ZrO_2–Al_2O_3$ sample nitnded in a three-stage heat treatment (850 °C for 1 h, 900 °C for 1 h and finally 950 °C for 1 h) are shown in Fig. 7. Fig. 7(a) is a micrograph of the edge of the sample. No nitridation appears to have taken place and the microstructure is identical to that of the preform sample. As we move into the sample, small regions where Si melting and recrystallization have taken place are visible, Fig. 7(b). These regions are visible throughout the bulk of the ceramic. These regions are up to 90 μm long and are found together in clusters or lines. In the centre of the sample, the area around these melted regions shows nitridation. At the edges of the sample, the area around these melted regions shows no nitridation. In the centre of the sample, larger melted and recrystallized regions are visible. In the center of the sample, the microstructure of the nitrided phase can be clearly seen,

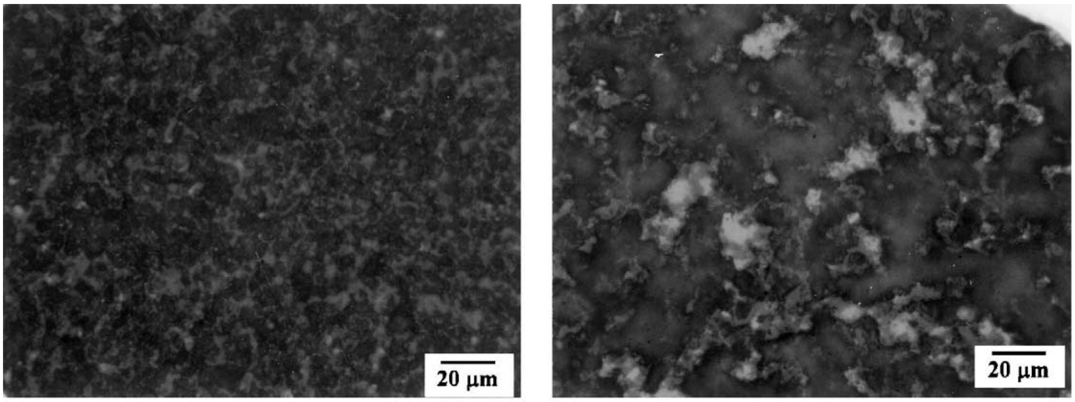

(a) (b)

Fig. 5. (a. Bulk of sample nitrided in multi stage treatment under 0.1 MPa pressure (850 °C for 1 h, followed by 900 °C for 1 h). (b) Centre of sample nitrided in multi stage treatment under 0.1 MPa pressure (850 °C for 1 h, followed by 900 °C for 1 h).

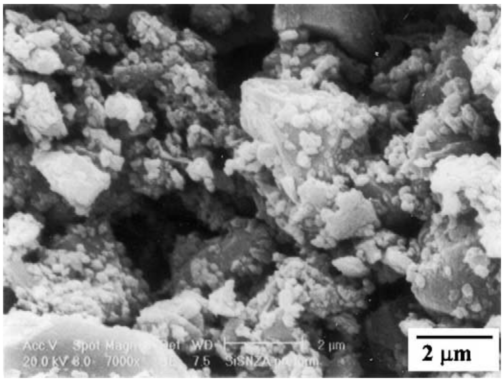

Fig. 6. Un-nitrided Si–Si_3N_4–ZrO_2–Al_2O_3 preform.

Fig. 7(c). The microstructure consists of a network of Si_3N_4 grains. XRD of this sample showed that both α- and β-Si_3N_4 are present (Fig. 11). Clusters of fine needles can also be seen. These are similar in appearance to the α-Si_3N_4 needles in the work of Jennings and Richman.[22] Macro (>1 µm) and micro (<1 µm) porosity is visible. Unreacted particles are also visible. These may be additive particles.

The Si–Si_3N_4–ZrO_2–Al_2O_3 samples are similar in microstructure to samples produced by Thomas et al.[23] Their samples also reacted from the surface inwards, and the middle of the samples reacted faster than the ends. In their samples large axial temperature gradients were present but large radial temperature gradients were not. However, in the samples nitrided in this study both axial and radial temperature gradients were present.

Like the samples in this study, their samples also showed non-uniform nitridation, alternating light and dark bands and melting. Fully nitrided areas of their samples were white in colour and had a lower density than partially nitrided areas, and no residual Si. Similarly, in this study white areas of the samples showed almost complete nitridation and greater amounts of porosity than dark areas. Thomas et al. suggested that the fully nitrided areas overheated. This caused excess Si vapor to form, which diffused away to other parts of the specimen or left the specimen entirely.

From electrical conductivity measures made on partially nitrided samples, Thomas et al.[23] proposed that as the green specimens began to nitride, the Si particles began to sinter and form necks between the particles. This increased particle–particle contact caused the specimen to become electrically conducting. Most of the microwave energy was then reflected instead of being absorbed, with the remainder being absorbed at the surface. As nitridation continued, the amount of particle–particle contact between Si particles decreased, causing the specimen to become electrically insulating. This allowed the specimen to absorb more microwave energy. Areas that had undergone more nitridation would absorb more energy than other areas, leading to large temperature gradients and overheating.

From the similarities in microstructure between the samples in this study and Thomas et al.'s samples, it appears that a similar chain of events is happening in the Si–Si_3N_4–ZrO_2–Al_2O_3 samples nitrided in this study. The use of an inverse temperature gradient makes control of the sample temperature more difficult, which leads to uneven nitridation and overheating within the samples.

3.6. X-ray diffraction

X-ray diffraction spectra of Si–Si_3N_4–ZrO_2–Al_2O_3 samples nitrided under 0.2 MPa pressure are shown in Fig. 8. The third sample in each batch (i.e. the sample that the pyrometer was focused on) was characterized by XRD. The phases present are listed in Table 2. The sample nitrided at 850 °C consists of Si as the major phase, with α-Si_3N_4, $Zr_7O_{11}N_2$/$Zr_7O_8N_4$ and ZrO_2 as minor phases. The sample nitrided at 860 °C contains the same phases, but the number of peaks for α-Si_3N_4 and $Zr_7O_{11}N_2$/$Zr_7O_8N_4$ have decreased.

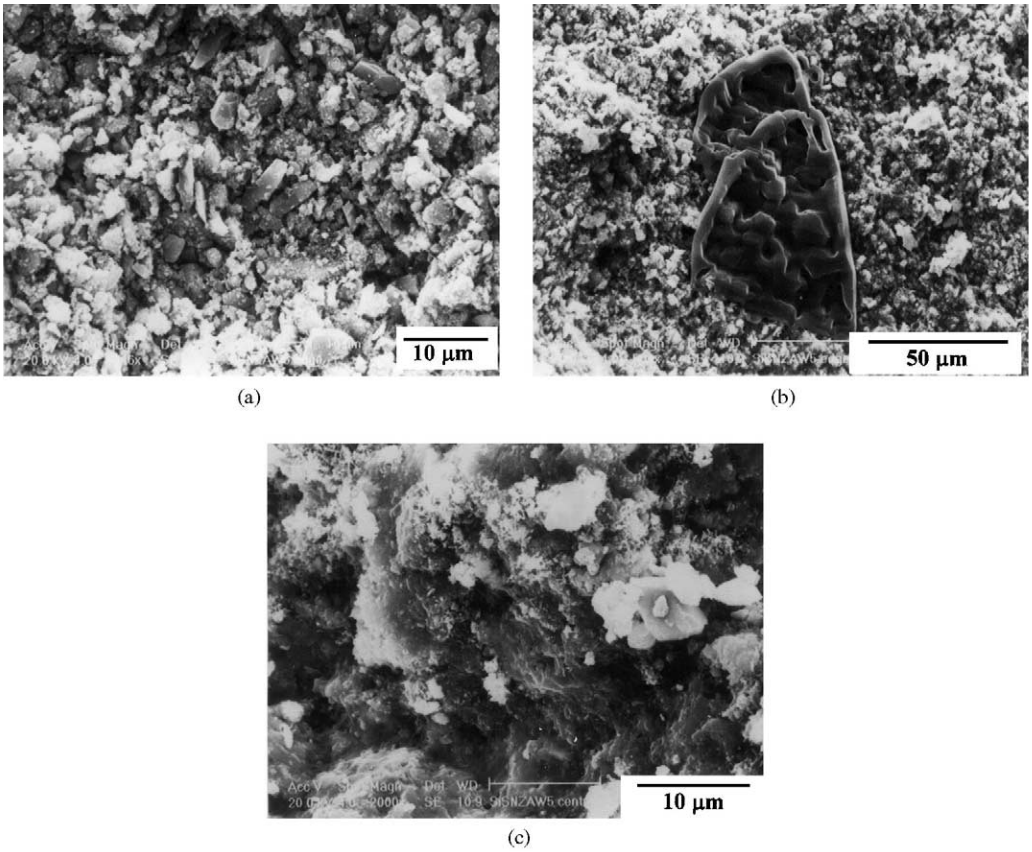

(a) (b)

(c)

Fig. 7. Nitrided Si–Si_3N_4–ZrO_2–Al_2O_3 sample (three stage treatment: 850 °C for 1 h, 900 °C for 1 h, 950 °C for 1 h): (a) Edge of sample; (b) melted and recrystallized regions in sample; (c) centre of sample.

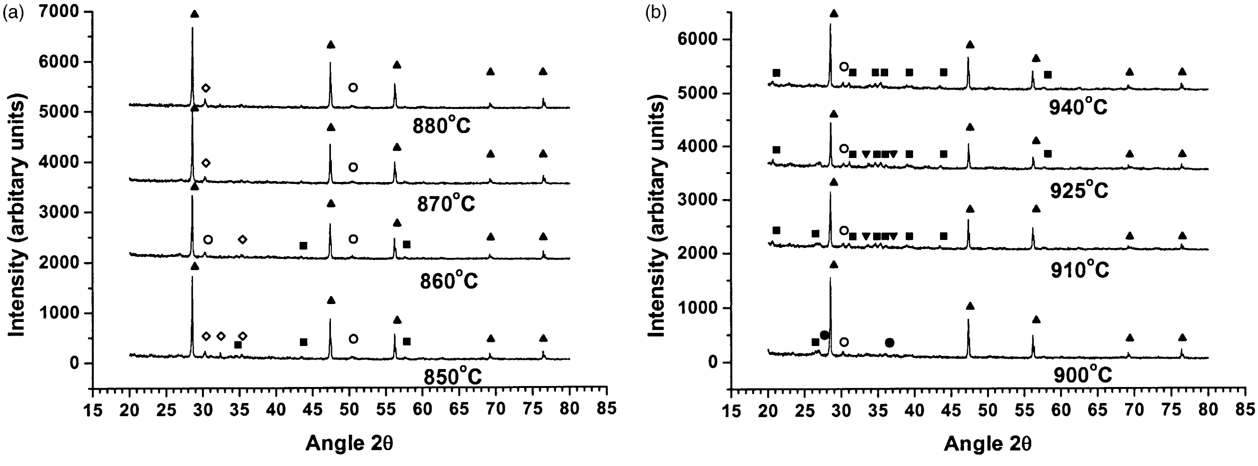

Fig. 8. (a) XRD pectra of nitrided Si–Si_3N_4–ZrO_2–Al_2O_3 samples (0.2 MPa pressure, single stage run): ▲ = Si; ■ = α-Si_3N_4; ◇ = $Zr_7O_{11}N_2$/$Zr_7O_8N_4$; ○ = ZrO_2. (b) XRD spectra of nitrided Si–Si_3N_4–ZrO_2–Al_2O_3 samples (0.2 MPa pressure, single stage run): ▲ = Si; ■ = α-Si_3N_4; ▼ = β-Si_3N_4; ● = Si_3AlON_7; ○ = ZrO_2.

For the samples nitrided at 870 and 880 °C, only peaks for Si, ZrO_2 and $Zr_7O_{11}N_2$/$Zr_7O_8N_4$ are present. $Zr_7O_{11}N_2$ and $Zr_7O_8N_4$ have very similar diffraction patterns so differentiating between the two was not possible. ZrO_2 also has a similar diffraction pattern to these two zirconia oxynitrides, further complicating assignment of peaks to a particular compound.

In the samples nitrided at temperatures ⩾900 °C, the zirconia oxynitride peaks have disappeared. In the sample nitrided at 900 °C, in addition to the peaks for Si and ZrO_2, peaks for Si_3AlON_7 are present. One α-Si_3N_4 peak is also present. In samples nitrided at 910 and 925 °C, the Si_3AlON_7 peaks have disappeared and have been replaced by peaks for α- and β-Si_3N_4. The sample

Table 2
Phases present in nitrided Si–ZrO_2–Al_2O_3 samples (0.2 MPa pressure, single stage run)

Temperature (°C)	Major phases	Minor phases
850	Si	ZrO_2, α-Si_3N_4, $Zr_7O_{11}N_2$/$Zr_7O_8N_4$
860	Si	ZrO_2, α-Si_3N_4, $Zr_7O_{11}N_2$/$Zr_7O_8N_4$
870	Si	ZrO_2,$Zr_7O_{11}N_2$/$Zr_7O_8N_4$
880	Si	ZrO_2,$Zr_7O_{11}N_2$/$Zr_7O_8N_4$
900	Si	ZrO_2, α-Si_3N_4, Si_3AlON_7
910	Si	ZrO_2, α-Si_3N_4, β-Si_3N_4
925	Si	ZrO_2, α-Si_3N_4, β-Si_3N_4
940	Si	ZrO_2, α-Si_3N_4

nitrided at 940 °C shows peaks for Si, ZrO_2 and α-Si_3N_4, but no peaks for β-Si_3N_4.

There are differences in the XRD spectra of samples within each batch. XRD spectra of samples nitrided at 900 °C are shown in Fig. 9. Sample 1 was the bottom sample in the stack; sample 3 was in the middle of the stack and sample 5 towards the top. In sample 1, Si is the major phase with minor phases of ZrO_2 and $Zr_7O_{11}N_2$/$Zr_7O_8N_4$ also present. In sample 3, Si is still the major phase but the $Zr_7O_{11}N_2$/$Zr_7O_8N_4$ phase has disappeared and peaks of Si_3AlON_7 and α-Si_3N_4 are present. In sample 5 Si, Si_2N_2O and β-Si_3N_4 peaks are present. The presence of Si_2N_2O is unusual, as the H_2 in the nitriding atmosphere should have made the formation of α-Si_3N_4 preferable over that of Si_2N_2O.[24]

XRD spectra of samples nitrided in multi-stage nitridation treatments are shown in Fig. 10. All the samples contain Si as the major phase. The sample nitrided at 850 °C has ZrO_2 and α-Si_3N_4 as minor phases. The other samples contain ZrO_2, α- and β-Si_3N_4 as minor phases. As the final nitridation temperature increases, the number of α-Si_3N_4 peaks also increases, whilst the number of β-phase peaks remains constant.

X-ray diffraction of the samples nitrided under 0.2 MPa pressure produced some unusual results (Fig. 8). Very little Si_3N_4 phase is formed until 910 °C, despite an apparent 28% nitridation of the sample. Instead oxynitride phases appear to be the main phases that are formed. Si–Al-oxynitrides can be formed by the reaction of the sintering aids and N_2 with the SiO_2 layer present in the surface of the Si particles. Zr oxynitrides can be formed by the ZrO_2 sintering aid reacting with N_2 gas. It must be remembered however that the samples in any particular batch do not nitride uniformly (Fig. 9). Rather, different compounds and different degrees of nitridation occur in each sample. Therefore it is difficult to determine the reactions that are taking place in the samples.

At temperatures of ⩾900 °C, Zr oxynitrides are not present. Zr oxynitrides are easily reoxidized to ZrO_2,[25] so any Zr nitride oxide formed could react with O_2 liberated by earlier nitridation reactions to produce ZrO_2.

In Fig. 9, it can be clearly seen that samples in different positions in the stack nitride to produce different compounds. This is due to temperature differences in the stack. The samples adjacent to the hole in the fiberboard (sample 3) were at a lower temperature than other samples in the stack.

The samples nitrided under 0.1 MPa (Fig. 10) contain no oxynitride phases, unlike samples nitrided under 0.2 MPa. Reducing the gas pressure has retarded the growth of the oxynitride phases. The lack of an oxynitride phase allows the growth of the α- and β-Si_3N_4 phases at 900 °C. This explains why the samples nitrided under 0.1 MPa pressure showed greater nitridation than samples nitrided under 0.2 MPa pressure.

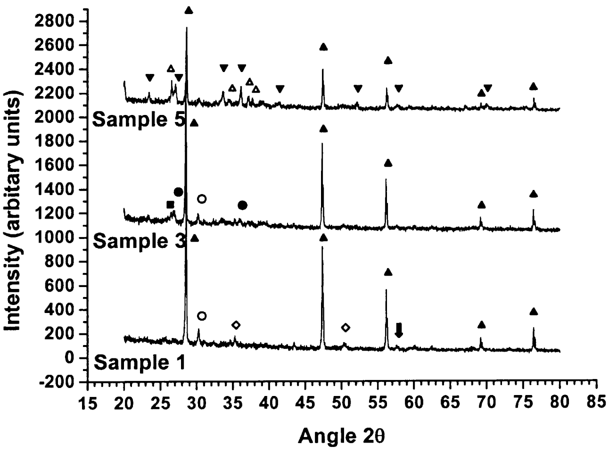

Fig. 9. XRD spectra of samples nitrided at 900 °C (0.2 MPa pressure, single stage run): ▲ = Si; ■ = α-Si_3N_4; ▼ = β-Si_3N_4; ○ = ZrO_2; △ = Si_2N_2O; ● = Si_5AlON_7 ; ◇ = $Zr_7O_{11}N_2$/$Zr_7O_8N_4$; ↓ = α-Al_2O_3.

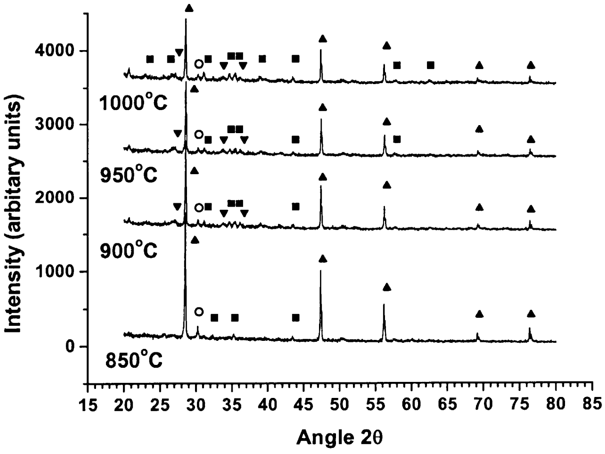

Fig. 10. XRD spectra of samples nitrided in multi-stage nitridation treatments (0.1 MPa pressure): ▲ = Si; ■ = α-Si_3N_4; ▼ = β-Si_3N_4; ○ = ZrO_2.

4. Conclusions

$Si–Si_3N_4–ZrO_2–Al_2O_3$ samples have been produced using an aqueous gelcasting technique. Samples up to 1 cm thick could be produced without cracking. These samples were nitrided in a microwave furnace to produce reaction bonded Si_3N_4. A vertical stack sample arrangement was used. Upto 40% nitridation was achieved by nitriding $Si–Si_3N_4–ZrO_2–Al_2O_3$ samples at 930–950 °C. Above this temperature the amount of nitridation began to decrease. ZrO_2 and Al_2O_3 appear to be unsuitable as sintering additives. Samples displayed an inverse temperature gradient. The edges of the samples did not react, whilst the centers tended to overheat, leading to evaporation or melting of Si. The use of an inverse temperature gradient made control of the sample temperature difficult, which led to uneven nitridation and overheating within the samples. Melting could be reduced by reducing the nitriding gas pressure, thereby slowing down the nitridation reaction. Samples nitrided in single-stage runs under 0.2 MPa pressure at temperatures from 850 to 900 °C formed α-Si_3N_4 and Al and Zr-containing oxynitride phases. Samples nitrided under 0.2 MPa pressure at temperatures greater than 900 °C formed α- and β-Si_3N_4 (Fig. 8b). Samples nitrided in multi-stage runs under 0.1 MPa pressure formed α- and β-Si_3N_4 at nitridation temperatures from 850 to 1000 °C. The unusual nitridation behavior of the samples nitrided in single stage runs under 0.2 MPa pressure may have been caused by the formation of Zr and Si–Al oxynitride phases. However, differences in composition between samples in the same batch make interpretation of the results difficult.

Acknowledgements

J.G. Fisher would like to thank the European Union for supporting this project under the European Union Science and Technology Fellowship Program in Korea (Contract No. ERB IC17 CT982097). The authors would also like to thank K.T. Im and D.S. Choi for their help with the experimental work, and Professor J.G.P. Binner for helping to arrange the project and for his advice.

References

1. Smyth, J. R., Advanced gas turbines. In *Ceramics and Glasses, Vol. 4, Engineered Materials Handbook*. ASM International, Metals Park, OH, 1991, pp. 905–1002.
2. Thomas, J. J., Christensen, R. J., Johnson, D. L. and Jennings, H. M., Nonisothermal microwave processing of reaction-bonded silicon nitride. *J. Am. Ceram. Soc.*, 1993, **76**(5), 1384–1386.
3. Tiegs, T. N., Kiggans, J. O. and Kimrey, H. D., Microwave processing of silicon nitride. In *Microwave Processing of Materials—II, Vol. 189*. Materials Research Soc., Pittsburgh, PA, 1990, pp. 267–272.
4. Kiggans, J. O., Hubbard, C. R., Steele, R. R., Kimrey, H. D., Holcombe, C. E. and Tiegs, T. N., Characterization of silicon nitride synthesized by microwave heating. In *Ceramic Transactions: Microwaves, Theory, and Applications in Materials Processing, Vols. 267–272*. Am. Ceram. Soc., Westerville, OH, 1991, pp. 665–671.
5. Tiegs, T. N., Kiggans, J. O. and Ploetz, K. L., Sintered reaction-bonded silicon nitride by microwave heating. *Mat. Res. Soc. Symp. Proc.*, 1993, **287**, 283–288.
6. Tiegs, T. N., Kiggans, J. O., Lin, H. T. and Willkens, C. A., Comparison of properties of sintered and sintered reaction-bonded silicon nitride fabricated by microwave and conventional heating. *Mat. Res. Soc. Symp. Proc.*, 1994, **347**, 501–506.
7. Tiegs, T. N., Kiggans, J. O. and Kimrey, H. D., Microwave sintering of silicon nitride. *Ceram. Eng. Sci. Proc.*, 1991, **12**(9–10), 1981–1992.
8. Gazza, G. E., Hot pressed silicon nitride. *J. Am. Ceram. Soc.*, 1973, **56**(12), 662.
9. Negita, K., Effective sintering aids for silicon nitride ceramics. *J. Mat. Sci. Lett.*, 1985, **4**, 755–758.
10. Cevales, G., *Ber. Deut. Keram. Ges.*, 1968, **45**(3), 217.
11. Xie, Z., Wang, C., Fan, X. and Huang, Y., Microwave processing and properties of Ce-Y-ZrO_2 ceramics with 2.45 GHz irradiation. *Materials Letters*, 1999, **38**(3), 38190–38196.
12. Rice, R. W. and McDonough, W. J., Hot pressed silicon nitride with Zr-based additions. *J. Am. Ceram. Soc.*, 1975, **58**(5–6), 264.
13. Messier, D. R. and Gazza, G. E., Thermal decomposition of alumina-silicon nitride mixtures. *J. Am. Ceram. Soc.—Discussions and Notes*, 1975, **58**(11–12), 538–540.
14. Weiss, J., Gauckler, L. J. and Tien, T. Y., The system silicon nitride-silica-zirconium nitride-zirconia. *J. Am. Ceram. Soc.—Discussions and Notes*, 1979, **62**(11–12), 632–634.
15. Inomata, Y., Hasegawa, Y., Matsuyama, T. and Yajima, Y., *Yogyo Kyokaishi*, 1976, **84**, 600–604.
16. Janney, M. A., Omatete, O. O., Watts, C. A., Nunn, S. D., Ogle, R. J. and Westmoreland, G., *J. Am. Ceram. Soc.*, 1998, **81**(3), 581–591.
17. Thomas, J. J., Christensen, R. J., Johnson, D. L. and Jennings, H. M., Nonisothermal microwave processing of reaction-bonded silicon nitride. *J. Am. Ceram. Soc.*, 1993, **76**(5), 1384–1386.
18. Maria, J. P., Kiggans, J. O., Tiegs, T. N. and Nunn, S. D., Gelcasting of sintered reaction bonded silicon nitride for improved mechanical properties. *Ceram. Eng. Sci. Proc.*, 1995, **16**(5), 1071–1075.
19. Moulson, A. J., Review-reaction bonded silicon nitride: its formation and properties. *J. Mat. Sci.*, 1979, **14**, 1017–1051.
20. Hackly, V. A., Paik, U., Kim, B. H. and Maighan, S. G., Aqueous processing of sintered reaction bonded silicon carbide: 1, dispersion of silicon powder. *J. Am. Ceram. Soc.*, 1997, **80**(8), 1781–1788.
21. Ziegler, G., Heinrich, J. and Wötting, G., Review—relationships between processing, microstructure and properties of dense and reaction bonded silicon nitride. *J. Mat. Sci.*, 1987, **22**, 3041–3086.
22. Jennings, H. M. and Richman, M. H., Structure, formation mechanisms and kinetics of reaction-bonded silicon nitride. *J. Mater. Sci.*, 1976, **11**, 2087–2098.
23. Thomas, J. J., Skamser, D. J., Jennings, H. M. and Johnson, D. L., Formation of reaction bonded silicon nitride using microwave heating. *J. Am. Ceram. Soc.*, 1996, **79**(9), 2458–2468.
24. Barsoum, M., Kangutkar, P. and Koczak, M. J., Nirtidation kinetics and thermodynamics of silicon powder compacts. *J. Am. Ceram. Soc.*, 1991, **74**(6), 1248–1253.
25. Terao, K., Miyamoto, Y. and Koizumi, M., *J. Am. Ceram. Soc.*, 1988, **71**(C-167/C-169).